Robust multi-objective optimization under multiple-uncertainties using CM-ROPAR approach: case study of the water resources allocation in the Huaihe River Basin

Jitao Zhang[1,2,3], Dimitri Solomatine[2,3,4], Zengchuan Dong[1]

[1]College of Hydrology and water resources, Hohai University; Nanjing, 210000, China.

[2]Water Resources Section, Delft University of Technology; Delft, 2628 CD, Netherlands.

[3]IHE Delft Institute for Water Education; Delft, 2628 AX, Netherlands

[4]Water Problems Institute of RAS, Moscow 119333, Russia

Correspondence to: Zengchuan Dong (zcdong@hhu.edu.cn)

Abstract. Water resources managers need to make decisions in a constantly changing environment because the data relating to water resources is uncertain and imprecise. The Robust Optimization and Probabilistic Analysis of Robustness (ROPAR) algorithm is a well-suited tool for dealing with uncertainty. Still, the failure to consider multiple uncertainties and multi-objective robustness hinder the application of the ROPAR algorithm to practical problems. This paper proposes a robust optimization and robustness probabilistic analysis method that considers numerous uncertainties and multi-objective robustness for robust water resources allocation under uncertainty. The Copula function is introduced for analyzing the probabilities of different scenarios. The robustness with respect to the two objective functions is analyzed separately, and the Pareto frontier of robustness is generated. The relationship between the robustness with respect to the two objective functions is used to evaluate water resources management strategies. Use of the method is illustrated on a case study of water resources allocation in the Huaihe River Basin. The results demonstrate that the method opens a possibility for water managers to make more informed uncertainty-aware decisions.

1. Introduction

Water resources is a natural resource necessary for human survival (Chen et al., 2017) but also a driving force for social and economic development (Dong and Xu, 2019). Due to the increasing population and rapid growth of economy, a contradiction between the supply and demand of water resources is becoming more acute, water quality problems are becoming more prominent, and water resources have gradually become a bottleneck for socio-economic development (Zhuang et al., 2018). This phenomenon is particularly evident in rapidly urbanizing and vital agricultural and industrial production watersheds (Yang et al., 2017). In this category of watersheds, agricultural and industrial production pose a massive challenge to water resource management (WRM) due to accelerated urbanization and rapid socio-economic development (Sun et al., 2019). River basin managers must consider water sources in an integrated manner and decide how to allocate water resources between different water-using sectors and cities within the basin (Xiong et al., 2020).

Multi-objective optimization (MOO) is an effective method for improving water resources allocation

(WRA) schemes (Lu et al., 2017; Abdulbaki et al., 2017). MOO can provide decision-makers with WRA options based on their preferences for objectives, which makes it a well-suited decision-making method for WRM. Ashofteh et al. (2013) constructed a bottom-line-based multi-objective optimization model to calculate WRA schemes. Habibi Davijani et al. (2016) presented a multi-objective optimal allocation model of water resources in arid areas based on maximum socioeconomic benefits. However, WRM is not only a multi-stage and multi-objective problem but also a complex problem involving uncertainties and risk management (Yu and Lu, 2018). WRM departments often need to face decision challenges under uncertain conditions (Hassanzadeh et al., 2016; Ren et al., 2019). Climate change and human activities have led to an increase in uncertainties in rainfall and water demand in the basin and hence to uncertainty in managing water resource systems (Jin et al., 2020; Ma et al., 2020; Zhu et al., 2019). Uncertain factors may lead to the risk of water shortage in the basin, so the existing WRA schemes may not be longer applicable (Keath and Brown, 2009). Therefore, it is important to study WRA under uncertainty.

Previously, several methods were introduced to analyze uncertainty in WRM. Scenario building and analysis is regarded as an effective method for considering possible future events and analyzing future uncertainties (Zeng et al., 2019). The fuzzy logic theory is one of the methods to deal with uncertainty, which describes uncertainty by fuzzifying the decision variables (Nikoo et al., 2013). Two-stage stochastic programming (TSP) is also an available planning method in optimization under uncertainty (Li et al., 2020). However, these approaches do not explicitly evaluate the robustness of the WRA options, although they take into account the uncertainties in WRA.

Robust multi-objective optimization (RMOO) is an effective method for forming robust WRA schemes. In relation to water, RMOO was actively applied in the field of water supply system (Kapelan et al., 2005; Kapelan et al., 2006). In the last decade, RMOO has been gradually applied to other areas of WRM. Yazdi et al. (2015) and Kang and Lansey (2013) applied robust optimization to design wastewater pipes by considering uncertainties such as climate change, urbanization, and population change. Marchi et al. (2016) formed stormwater harvesting schemes under variable climate conditions using RMOO. It should be pointed out however, that in the mentioned approaches the robustness is often “hidden” into the objective function or constraints and then a common MOO problem is solved that forms a single Pareto front. This is indeed an effective method to create solution set which in a certain sense is robust. However, this approach does not explicitly show the relationship between the solution and the uncertainty variables, which prevents the decision-maker from clearly understanding the impact of uncertainty, which can influence the decision. To answer this limitation, the procedure “Robust Optimization and Probabilistic Analysis of Robustness” (ROPAR) has been developed and presented first in (Solomatine, 2012). The method will generate multiple Pareto fronts, each corresponding to a sample of uncertain variables so that the statistical characteristics of the uncertainty of the solution can be analyzed. The ROPAR has been applied in the design of urban stormwater drainage pipes (Solomatine and Marquez-Calvo, 2019) and for water quality management in water distribution (Marquez Calvo et al., 2019; Quintiliani et al., 2019).

To the best of our knowledge, the presented versions of the ROPAR methodology have the following limitations: (1) ROPAR method has not been applied to the field of WRA; (2) ROPAR method only considers the single source of uncertainty: if there are two sources, then the joint probability of these sources needs to be considered; (3) ROPAR method only analyses the variability of one objective under conditions where the other objective function level is fixed. Although the ROPAR method can provide decision-makers with a robust solution under certain conditions, it does not take into account the relationship between the two objective functions.

Based on the above analysis, although the ROPAR method has proven to be suitable for dealing with uncertainty, it still needs improvement. In this study, we propose a Copula-Multi-objective Robust Optimization and Probabilistic Analysis of Robustness (CM-ROPAR) procedure under multiple uncertainties for WRA. The proposed new procedure of the ROPAR-family considers the joint probability distribution of uncertainties (in this case, inflows) and enables decision-makers to check the robustness of the two objective functions separately.

The following text is structured as follows. First, the Chapter 2 presents the methodology of the paper. It mainly includes the method of Copula function, the method of CM-ROPAR algorithm, the definition of robustness and the construction of water resources allocation model. Then, the Chapter 3 introduces the overview of the study area. Then, the Chapter 4 introduces the application examples of CM-ROPAR algorithm, and this paper is an example of water resources allocation of Huaihe River Basin. Finally, the last Chapter introduces the conclusion of the paper.

2. Methodology

2.1 Method of Copula Function

Sklar proposed Copula theory in 1959, in which he decomposed an N-dimensional Joint Distribution Function (JDF) into a Copula function and N Marginal Distribution Functions (MDF), which are not required to be the same distribution for N variables and can be used to describe the correlation between arbitrary variables. Nelsen discussed the basic properties and some of the main applications of Copula functions in 1999 (Nelsen et al., 2008). Copula function is the function that connects the JDF with their respective MDF. Copula functions can be expressed as:

$$C_\theta(u_1, u_2 \ldots u_n) = C_\theta[F_1(x_1), F_2(x_2) \ldots F_n(x_n)] \quad (1)$$

where $x_1, x_2 \ldots x_n$ are random vectors, $u_1 = F_1(x_1), u_2 = F_2(x_2) \ldots u_n = F_n(x_n)$ are MDF of the random vectors, θ is the parameter or the parameter vector of copula function.

The basic copula functions are mainly classified into Archimedean, elliptic, and quadratic types. Among them, Archimedean Copula functions have been widely applied in the field of hydrology(Salvadori et al., 2007). The Archimedean Copula multidimensional joint distribution models are the following:

(1) GH-Copula joint distribution model

$$C_\theta(u_1, u_2 \cdots u_n) = exp\left[-(\sum_{i=1}^{n}(-\ln u_i)^\theta)^{\frac{1}{\theta}}\right] \ (\theta > 1), \quad (2)$$

(2) Clayton Copula joint distribution model

$$C_\theta(u_1, u_2 \cdots u_n) = \left[1 + \sum_{i=1}^{n}(u_i{}^{-\theta} - 1)\right]^{-\frac{1}{\theta}} \ (\theta \in [-1,\infty)\backslash\{0\}), \quad (3)$$

(3) Frank Copula joint distribution model

$$C_\theta(u_1, u_2 \cdots u_n) = -\frac{1}{\theta} ln\left[1 + \frac{\prod_{i=1}^{n}(e^{-\theta u_1} - 1)}{(e^{-\theta} - 1)^{n-1}}\right] \ (\theta \in R\backslash\{0\}), \quad (4)$$

In a river basin, there may be different drought or wet conditions between different intervals of inflow, so the probability of drought and wet encounters between different intervals of inflow needs to be investigated. According to the analysis in Section 2.1, it is known that Copula function can be used to

construct the multivariate joint distribution function. Therefore, this paper adopts Copula function theory to construct the joint distribution and analyze the drought and wet encounter probability. The steps of Copula function-based wet-dry encounter analysis are as follows: 1. Fit and Select the MDF. The widely applied probability distribution functions are mainly Pearson type 3 distribution (P-III), T-distribution, Normal distribution, etc. MDF can be fitted by Maximum Likelihood Estimation method (MLE method) and the goodness-of-fit test can be performed by the Kolmogorov-Smirnov test (K-S test) and the Root Mean Square Error value (RMSE value). 2. Fit and Select Copula distribution function. Based on the MDF fitted in the first step, construct the Copula function and select the fitted Copula function by AIC and BIC criteria. 3. Calculate the probability of a dry and wet encounters between different interval inflows.

2.2 Method of CM-ROPAR

The basic flow of CM-ROPAR algorithm is shown in Figure 1. Firstly, the multi-objective optimization problem is defined and the uncertainty variables are clarified; secondly, the Copula function is used to analyze the relationship between the two sources of uncertainty; and finally, through sampling and multi-objective optimization calculations, the robustness of each solution is identified and the one with the most comprehensive robustness is selected.

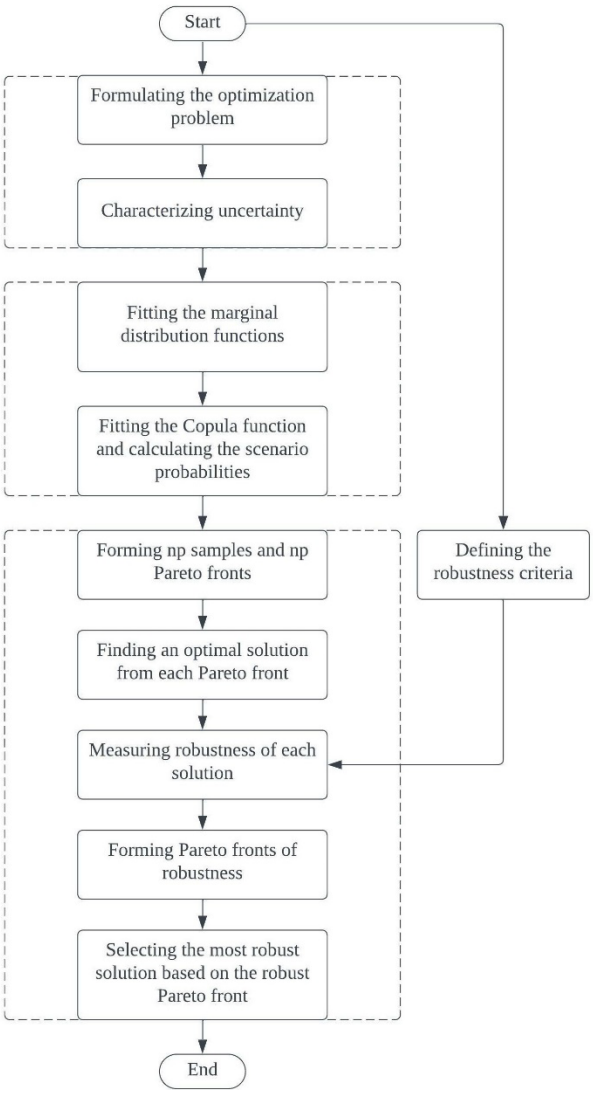

Figure 1. Flowchart of CM-ROPAR.

The specific process of optimal water allocation under runoff uncertainty based on MROPAR algorithm is as follows.

Part 1 (Analyzing the wet-dry encounters)

1.Analyze the inflow wet and dry encounters. If the basin has k inflows, then there are 3^k wet-dry scenarios. For example, suppose there is one inflow in the upper and one in the middle reaches of the basin. In that case, there are 9 scenarios: wet-medium, wet-wet, medium-wet, medium-medium, medium-dry, dry-wet, dry-medium, and dry-dry.

2.Choose a scenario from 1 to 3^k.

Part 2 (Sampling-Inflow)

3.Based on the recorded annual inflow data Q, it is assumed that Q is not a definite value but

$$Q = i_{uncertainty} * Q, \tag{5}$$

$$i_{uncertainty} \sim N(\mu, \sigma^2), \tag{6}$$

where $i_{uncertainty}$ follows a normal distribution.

4.For $i = 1 \ldots np$ do

5.Sample u (inflow). As mentioned before, the uncertainty variable is obtained from the normal

distribution $N(\mu, \sigma^2)$. Assuming that the uncertainty variable follows $N(1,0.0025)$,this represents that a 99.74% probability of the uncertainty variable falling within the interval $[0.85,1.15]$ and the inflow sample falling within the interval $[0.85 * Q, 1.15 * Q]$.

Part 3 (Forming the optimal solution set through np Pareto fronts)

7.Select an ideal solution (IS) in each Pareto front F_r based on the distance to the origin point, forming the optimal solution set (set S).

Part 4 (Evaluate the robustness of each solution)

8.Select a solution s_i $(i = 1 \ ... \ np)$ from the solution set S.

9.Cast the inflow case u_r $(r = 1 \ ... \ np)$ into s_i and calculate $P_r(u_r, s_i)$ and $WD_r(u_r, s_i)$, respectively, to form 1200 values of P_r and WD_r $(r = 1 \ ... \ np)$.

10.Select the robustness evaluation criteria, $RC1, RC2, RC3, RC4$.

11.For each s_i $(i = 1 \ ... \ np)$, calculate the $RC1, RC2, RC3, RC4$ and SRI corresponding to P_r and WD_r respectively. Plot the corresponding graphs and find the Pareto front of each graph.

12.Find the solution with the highest robustness.

End

2.3 Defining the robustness criteria

According to the general definition of robustness, four common Robustness Criteria (RC) were used in this study (Beyer and Sendhoff, 2007). These must be minimized to achieve the maximum robustness of the solution, so the lower the criteria, the higher the robustness.

For the four RC, two MOO are implicitly defined, and optimization can be named Two Layer-Multi-objective optimization of Robustness Criteria (TL-MOORC). It is worth noting that TL-MOORC differs from the problem's MOO. A one-layer MOORC is a solution that may not be minimized at all four RC simultaneously. This problem can be solved by aggregating the four RC into one, for example, using a linear weighted combination. The second layer of MOORC is that for the two objective functions of a solution, the RC for both objective functions may not be minimized at the same time. Therefore, a trade-off must be made between theRC for the two objective functions.

The first RC is the expected value of each objective function, denoted as $RC1$. It reflects the fact that we want to find a solution that is good on average across all uncertainties and can be represented by:

$$RC1(s) = \int_{N(s,u)} f(s,u)\, p(u) du, \tag{7}$$

Where is the probability density function of the uncertain variable u; it is the neighborhood of the solution s.

The second RC is the 'worst case' (or 'minimax' case), denoted as $RC2$. This RC is related to robustness because we want to find a solution s such that the value of each objective function in the worst case is the minimum possible. It can be presented as follows:

$$RC2(s) = \min\left(\max_{N(s,u)}\left(f(s,u)\right)\right), \tag{8}$$

The third RC is the 'standard deviation' of each objective function, denoted as $RC3$. $RC3$ is related to the robustness of each objective function because we want to find a solution S such that the value of the objective function would not vary too much due to uncertainty. It can be expressed as follows:

$$RC3(s) = \sqrt{\int_{N(s,u)} \left(f(s,u) - f(u)\right)^2 p(u) du}, \tag{9}$$

The fourth RC is the "probabilistic threshold", denoted as $RC4$. We want to find a solution s that minimizes the probability that the objective function is higher than the threshold of interest q. This

criterion is usually associated with the reliability of the system. It can be expressed as follows:

$$RC4(s) = Pr(f(s,u) > q|s), \quad (10)$$

In order to evaluate the integrated robustness of the water resources allocation scheme, the weighted sum of the four Normalized RC $(NRCi)$ in this study was used as the integrated robustness criteria. In this study, we consider that the four RC to be of equal importance, so all four indicators are given a weight of $\frac{1}{4}$.

$$SRI = \frac{1}{4}NRC1 + \frac{1}{4}NRC2 + \frac{1}{4}NRC3 + \frac{1}{4}NRC4, \quad (11)$$

(of course, other ways of aggregation can be considered as well.)

2.4 Construction of WRA Model

Objective function

（1） Social Goals: Water Deficit (WD)

$$minf_1(Q) = \sum_{j=1}^{J}\sum_{k=1}^{K}\left(\frac{D_{jk}-\sum_{t=1}^{T}\sum_{i=1}^{I}Q_{ijkt}}{D_{jk}}\right)^2, \quad (12)$$

Where D_{jk} denotes the water demand of the water consumption department k of the city j. $Q_{ijkt}$is the water supply quantity of water source $i$to water consumption department k of the city j in the period t.

（2） Ecological goals: Pollution (P)

$$minf_2(Q) = \sum_{j=1}^{J}\sum_{k=1}^{K} d_{jk}p_{jk}\sum_{i=1}^{I}\sum_{t=1}^{T}Q_{ijkt}, \quad (13)$$

Where d_{jk} denotes the representative pollutant discharge per unit of wastewater of the water department k of calculation unit j (ton/m^3) and p_{jk} represents the sewage discharge coefficient of the water consumption department of calculation unit. Discharge coefficient of water consumption department k of calculation unit j. Q_{ijkt} is the water supply quantity of water source i to water consumption department k of calculation unit j in the period t.

Constraints

（1） Water demand constraint

$$\sum_{i=1}^{I}\sum_{t=1}^{T}Q_{ijkt} \le D_{jk}, \quad (14)$$

（2） Water supply capacity constraint

$$\sum_{k=1}^{K}\sum_{j=1}^{J}\sum_{t=1}^{T}Q_{ijkt} \le U_{i}, \quad (15)$$

（3） Water Resources Constraint

$$\sum_{j=1}^{J}\sum_{k=1}^{K}Q_{ijk} \le WR_i, \quad (16)$$

3. Study Area Overview

The Huaihe River Basin is located in the eastern part of China, and as shown in Figure 2, the middle and upper basin flows through 15 cities of Henan Province and Anhui Province. It is an important agricultural and industrial production base in China (Xu et al., 2019). As shown in the Figure 3, the inflow of the Huaihe River Basin varies significantly between different years and between different regions, and the water demand is uneven among cities. In this study, water demand is calculated by using the quota method commonly used in the field of water resources. In addition, due to the discharge of pollutants, the contradiction between supply and demand of water resources in the middle and upper reaches of the Huaihe River Basin has become increasingly fierce. Therefore, it is meaningful to study the optimal

allocation of water resources and propose a robust water resources allocation scheme based on the wet-dry encounters in the Huaihe River Basin.

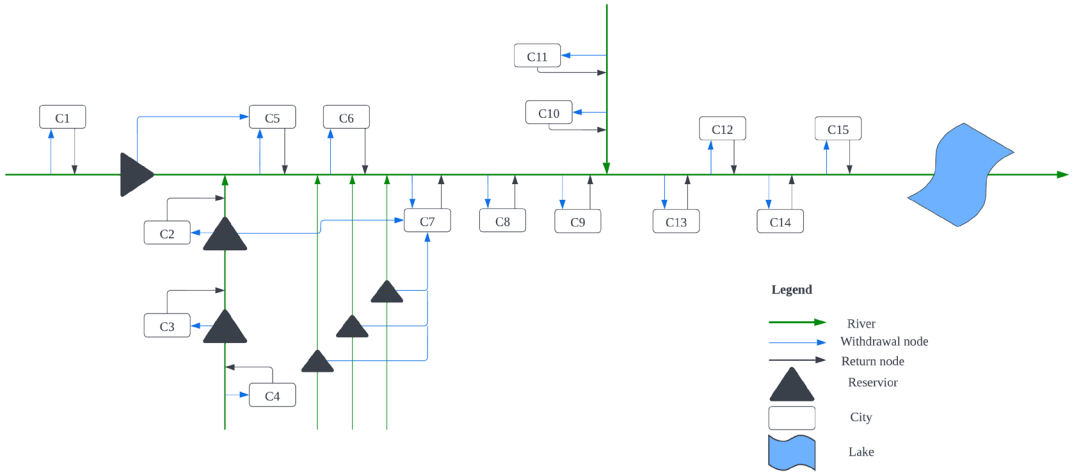

Figure 2. Overview of watershed water supply.

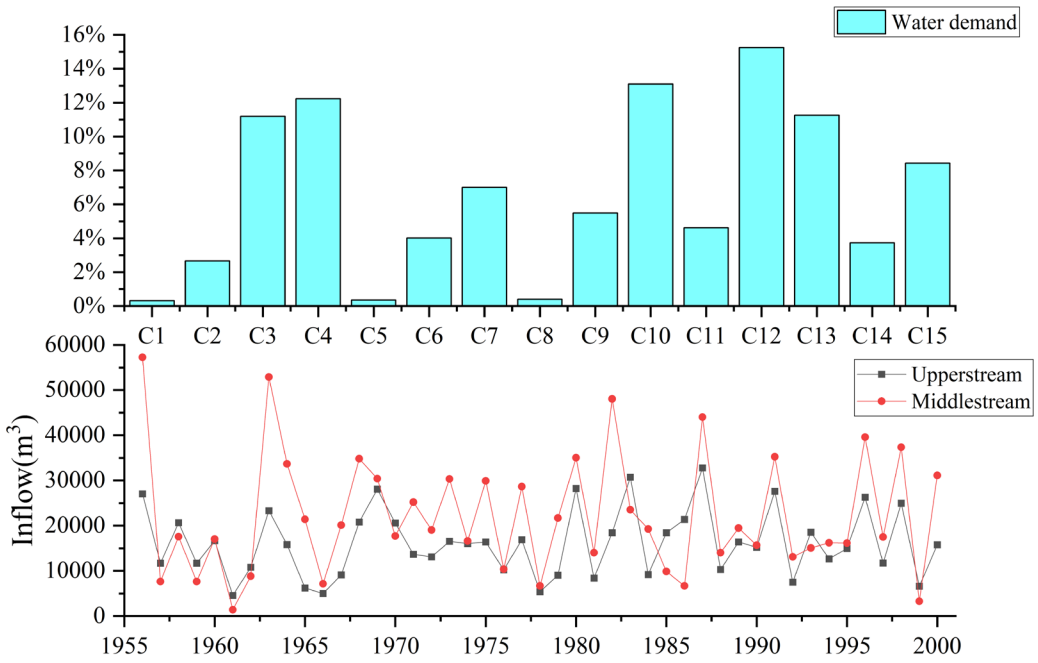

Figure 3. Water demand proportion and inflow historical data.

4. Results and discussion

4.1 Identification of marginal distribution functions

According to the first part (step 1-2) of the CM-ROPAR process, we need to construct the joint probability distributions for the upstream and midstream inflow and generate nine inflow scenarios via the Copula function. Therefore, before constructing the JDF, we need to construct the MDF for the

upstream and midstream inflows respectively. As shown in Table 1, based on the K-S test results and RMSE value, we found that the best-fitting distributions for the upstream and midstream were the Weibull and P-III distributions, respectively.

Table 1. MDF goodness-of-fit test results.

	Distribution type	Upper stream inflow	Middle stream inflow
p-value	Normal	0.3341	0.8637
	Log-normal	0.5175	0.5703
	P-III	**0.7674**	0.7599
	Weibull	0.5758	**0.9658**
	Rayleigh	0.6123	0.2173
D-value	Normal	0.13721	0.086144
	Lognormal	0.11821	0.1152
	P-III	**0.0958**	0.0965
	Weibull	0.1129	**0.0708**
	Rayleigh	0.1096	0.1533
RMSE	Normal	0.0345	0.0522
	Lognormal	0.1391	0.1152
	P-III	**0.0306**	0.0358
	Weibull	0.0929	**0.0306**
	Rayleigh	0.0529	0.1736

4.2 Analysis of upstream and midstream dry and wet encounters

The optimal Copula function is selected by comparing the Akaike information criterion (AIC) and the Bayesian information criterion (BIC), AIC and BIC values in Table 2. It can be concluded that the joint distribution function of the upper and middle reaches of the Huaihe River Basin is consistent with the joint distribution of the Clayton Copula function.

Table 2. AIC and BIC values for Copula functions.

	Gaussian	t	Clayton	Gumbel	Frank
AIC	-20.86	-18.34	**-22.69**	-12.47	-20.03
BIC	-19.06	-14.73	**-20.88**	-10.67	-18.22

Substituting the multi-year annual inflow for the upper and middle reaches of the Huaihe River Basin into the Clayton Copula function, respectively, the following results were obtained.

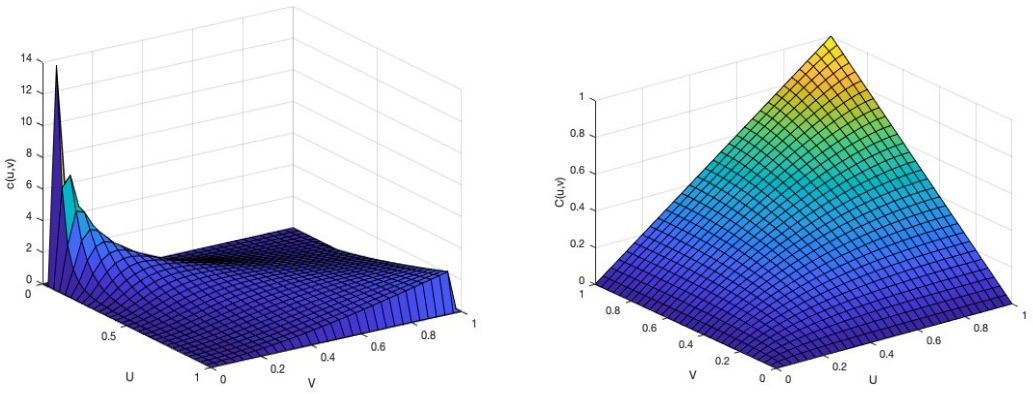

a b

Figure 4. Clayton Copula function.

As shown in Figure 4, the joint distribution of the annual incoming water in the upper and middle reaches of the Huaihe River Basin has symmetry. In addition, the joint distribution of annual water in the upper and middle reaches has a tail correlation, which indicates a higher probability of simultaneous wetness or drought in the upper and middle reaches.

Table 3. The probabilities of 9 scenarios.

Wet and Dry encounters/%		Upstream		
		Wet	Medium	Dry
Middlestream	Wet	27.7	7.8	5.3
	Medium	11.6	6.5	4.6
	Dry	4.6	7.8	24.1

As shown in Table 3, the probability of drought-wetness synchronization in the upper and middle reaches of the Huaihe River Basin is 58.3%, while the probability of asynchrony is 41.7%. The former is 16.6% higher than the latter, indicating that the upper and middle reaches are less able to complement each other. The joint distribution has a maximum probability of 27.7% that the upstream and midstream are both wet, and the risk of water scarcity is minimal under this scenario. The joint distribution has the second-highest probability of both upstream and midstream being dry at 24.1%, with the highest risk of water scarcity under this scenario.

4.3 Considering solutions for the uncertainty of inflow through MROPAR

In this study the situation when the upper and middle reaches are both wet is considered as a case study. For deterministic optimization we opted for the NSGA-II algorithm, which is widely used and has good historical performance (Reed et al., 2013). Inflow uncertainty is modelled by sampling 1200 inflows, as shown in Figure 5. In this study, NSGA- II algorithm is used for multi-objective function solving. For algorithm parameterization, the population size is 100, generation is 1000, cross rate is 0.9 and mutate rate is 0.2.

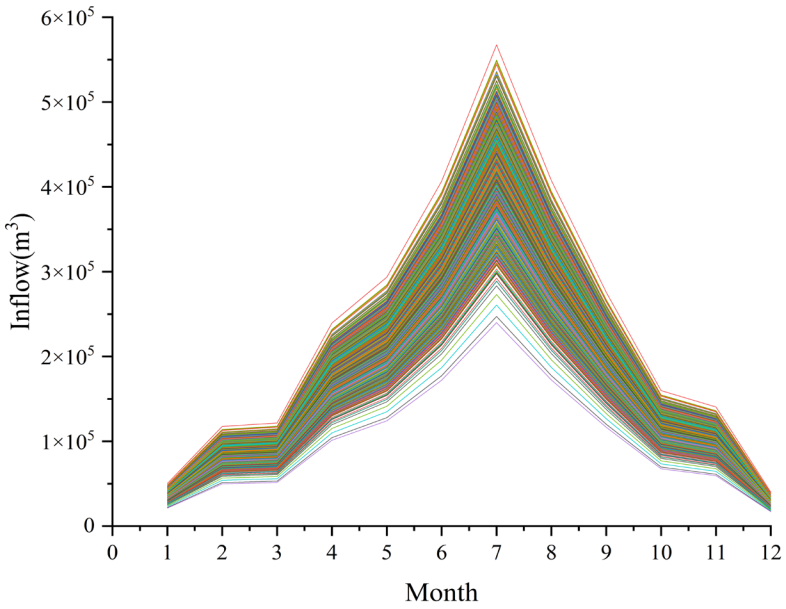

Figure 5. Inflow samples.

Figure 6(a) shows that 1200 Pareto fronts calculated for each sampled inflow, through steps 3-6 of CM-ROPAR. Figure 6(b) shows 1200 ideal solutions s, selected based on their distance to the ideal solution (step 7 of CM-ROPAR).

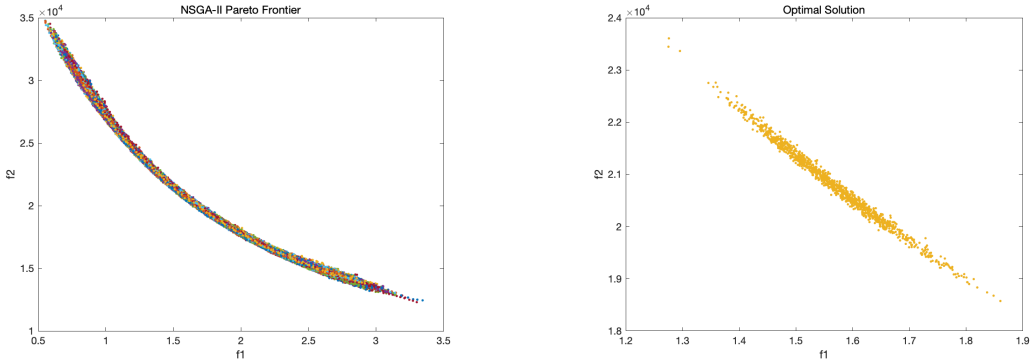

a b

Figure 6. a: 1200 Pareto fronts (f1: water deficit; f2: pollution) and b: 1200 ideal solutions (f1: water deficit; f2: pollution) selected based on their distance to the ideal solution.

4.4 Assessing robustness of the solutions found by CM-ROPAR

Four robustness criteria are calculated for each solution s in the solution set S. Given the solution s to be evaluated, it is necessary to calculate $WD(s, IF_r)(r = 1 \dots np)$ and $P(s, IF_r)(r = 1 \dots np)$ in order to calculate the four robustness criteria, where IF_r is the $rt\hbar$ sample of inflow. r depends on the number of samples; in this study, 1200 samples were taken, so np is 1200.

As shown in Table 4 and Figure 7, $RC1, RC2, RC3, RC4$ and SRI for WD and P can be calculated for each solution in S, and the solutions corresponding to the smallest value in each RCi and the solutions corresponding to the smallest value in SRI can be identified, respectively. In addition, we also feed 1200 samples to the deterministic solution and calculate $RC1, RC2, RC3, RC4$ and SRI for WD and P.

Table 4. Optimal solution numbers for different robustness criteria.

	$RC1$	$RC2$	$RC3$	$RC4$	SRI
WD	535	361	361	361	361
P	876	876	876	876	876
IS	629	84	84	915	84

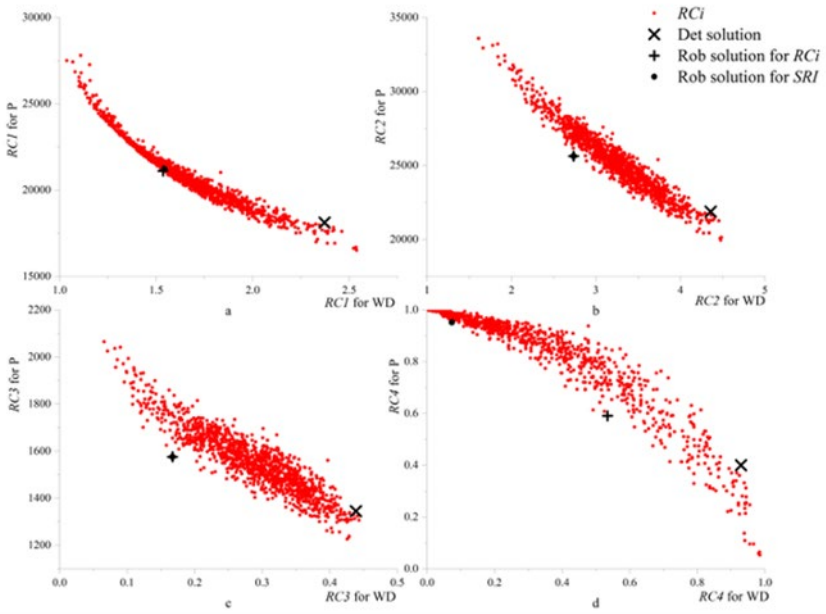

Figure 7. Performance of the robustness of solutions (a: $RC1$, b: $RC2$, c: $RC3$, d: $RC4$): robust model solutions (red dots), deterministic model solution (black ×), solution closest to origin for RCi (black +), solution closest to origin for SRI (black dot). The horizontal axis represents the performance of the robustness for WD. The vertical axis represents the robustness performance for P.

Figure 7 shows the performance of 1200 robust model solutions (red dots) and one deterministic model solution (black ×), for the four robustness criteria. From Figure 7, four Pareto fronts can also be found, which indicate the competitive relationship between water deficit and pollution emissions for each robustness criterion dimension. As shown in Figure 7(a), we can observe an interesting phenomenon that the left-most extreme solution (red dot) has the smallest robustness index $RC1$ for water deficit, but the highest robustness index $RC1$ for pollution; the right-most extreme solution (red dot) has the largest robustness index $RC1$ for water deficit, but the smallest robustness index $RC1$ for pollution. Similarly, this phenomenon can be also observed for the robustness criteria $RC2$, $RC3$, and $RC4$. More importantly, as shown in Table 4, the extreme solutions and the solutions closest to the origin point may differ for different robustness criteria. Specifically, for $RC1$, solution No. 535 is the most robust for water deficit, and solution No. 876 is the most robust for pollution; for $RC2$, $RC3$, and $RC4$, the most robust solution for water deficit is solution No. 361, and the most robust solution for pollution is solution No. 876.

Because there are many non-inferior solutions in the Pareto frontier, the decision-makers must choose among them. The decision-makers need not only to choose among the non-inferior solutions but also to evaluate the trade-off between different robustness criteria or to choose the best one by combining the criteria. This study takes the distance to the origin as the basis for such choice. As shown in Table 4,

for $RC1$, $RC2$, $RC3$, and $RC4$, the closest points to the origin are solution No. 629, solution No. 84, and solution No. 915, respectively.

4.5 Comparing solutions found by deterministic and robust approaches

To see a more general relationship between the 1201 solutions (i.e., 1200 from the robust optimization solution and 1 from the deterministic optimization solution), the performance of each solution for water deficit and pollution on each of the four robustness criteria (sorted from smallest to largest) is plotted in Figure 8 and Figure 9.

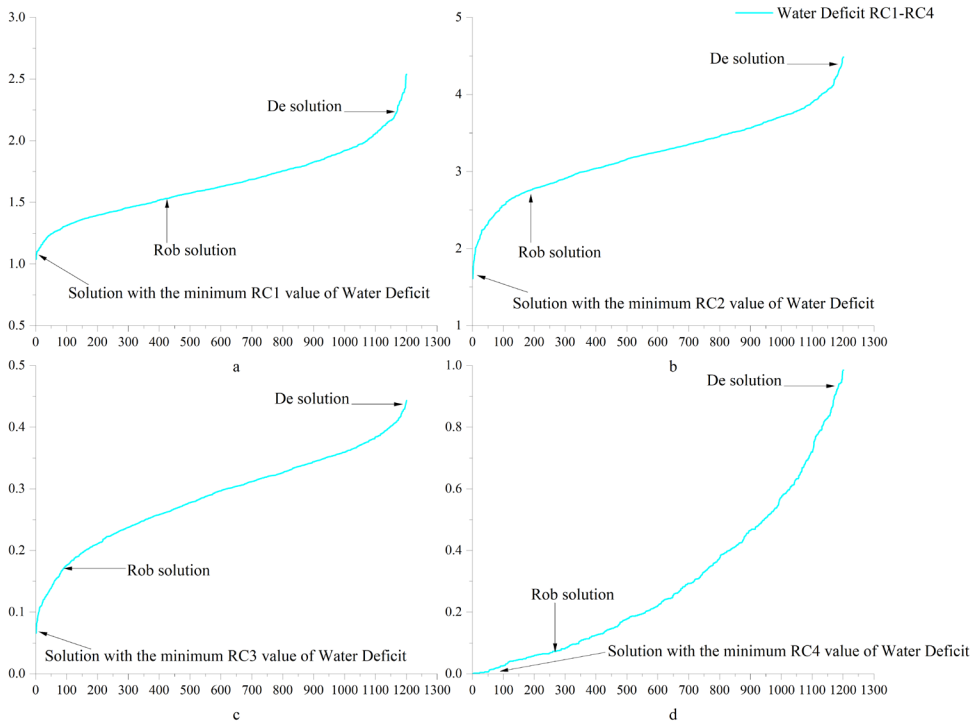

Figure 8. Robustness of water deficit (a: $RC1$, b: $RC2$, c: $RC3$, d: $RC4$). The horizontal coordinate represents the number of solutions and the vertical coordinate represents the robustness of the solution.

As shown in Figure 8, for water scarcity, the robust solution performed significantly better than the deterministic solution. Specifically, for the four robustness criteria, the robust solution outperforms 63.1%, 85.6%, 92.7%, and 77.7% of the solutions, respectively, while the deterministic solution outperforms only approximately 1% of the solutions. To analyze the robust and deterministic solutions more accurately and intuitively, this study applied the ratio of $RC(Det)/RC(Rob)$ to compare the robustness of the two solutions. The ratios of $RC(Det)/RC(Rob)$ are 1.53, 1.59, 2.62, and 12.67 in the four robustness criteria dimensions. This means that, regarding water deficit, the deterministic model solution may lead to 53%, 59%, 162%, and 1167% more variability in the four robustness criteria dimensions.

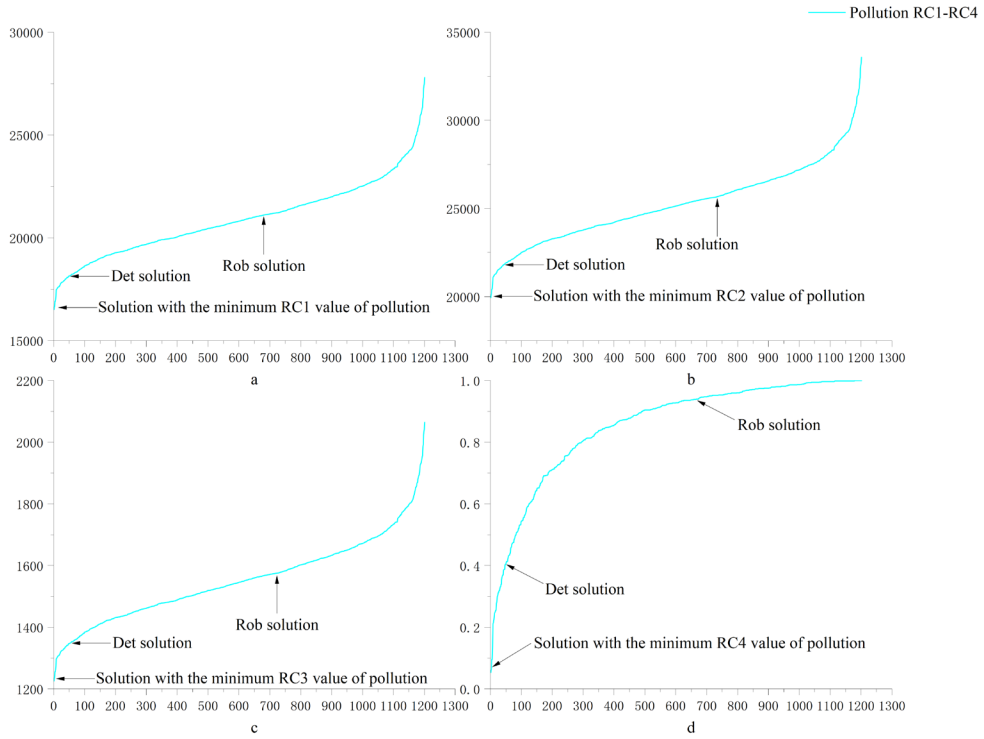

Figure 9. Robustness of pollution (a: $RC1$, b: $RC2$, c: $RC3$, d: $RC4$). The horizontal coordinate represents the number of solutions and the vertical coordinate represents the robustness of the solution.

However, as shown in Figure 9, the deterministic solution slightly outperforms the robust solution for pollution. Specifically, for the four robustness criteria, the deterministic solution outperforms 96% of the solutions, respectively, while the robust solution outperforms about 40% of the solutions. Similarly, we compare the two solutions by the ratio of $RC(Rob)/RC(Det)$. We find that the $RC(Rob)/RC(Det)$ ratio is about 1.17 for $RC1$ to $RC3$ and 2.37 for $RC4$. This means that, in terms of pollution, the robust solution may lead to 17% more variability for $RC1$ to $RC3$ and 137% more variability for $RC4$.

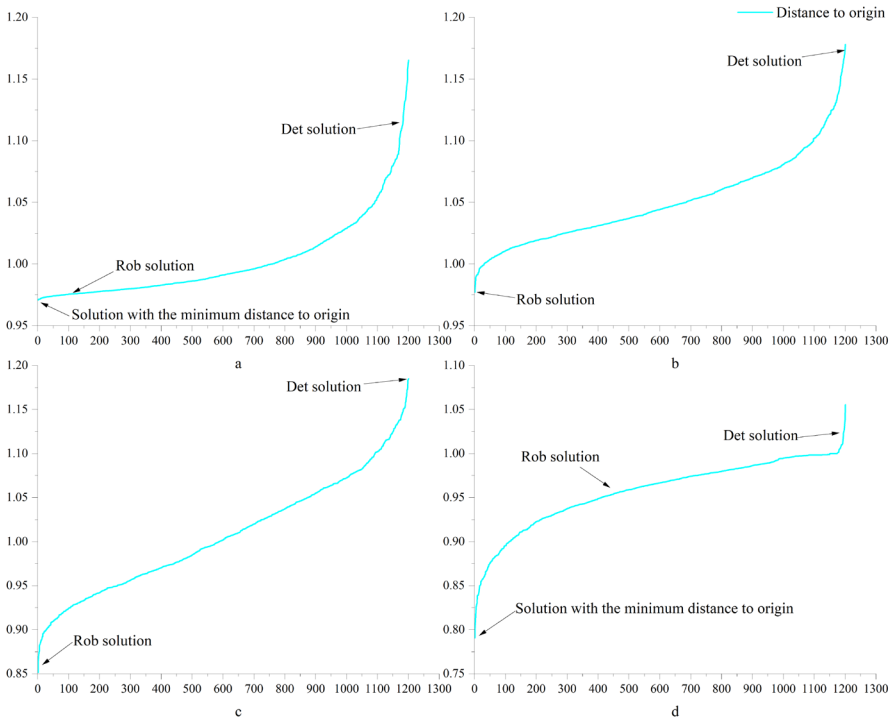

Figure 10. Comprehensive robustness for four indicators (a: $RC1$, b: $RC2$, c: $RC3$, d: $RC4$). The horizontal coordinate represents the number of solutions and the vertical coordinate represents the robustness of the solution.

In order to analyze the comprehensive performance of each solution, rather than just the robustness of a single objective, this study reflects the comprehensive implementation of each solution in terms of the distance from the solution to the origin. As shown in Figure 10, the comprehensive performance of the robust solution for $RC1$ to $RC4$ is significantly better than that of the deterministic model solution. Specifically, the robust solution outperforms 90.3% and 62.2% of the solutions in $RC1$ and $RC4$, respectively, and outperforms all solutions in $RC2$ and $RC3$, while the deterministic solution performs exceptionally poorly in all four robustness criteria. According to the ratio of $Dis(Rob)/Dis(Det)$, we can find that the robust solution is 16.8%, 19.8%, 39.2%, and 7.3% more robust than the deterministic solution in the four robustness dimensions, respectively.

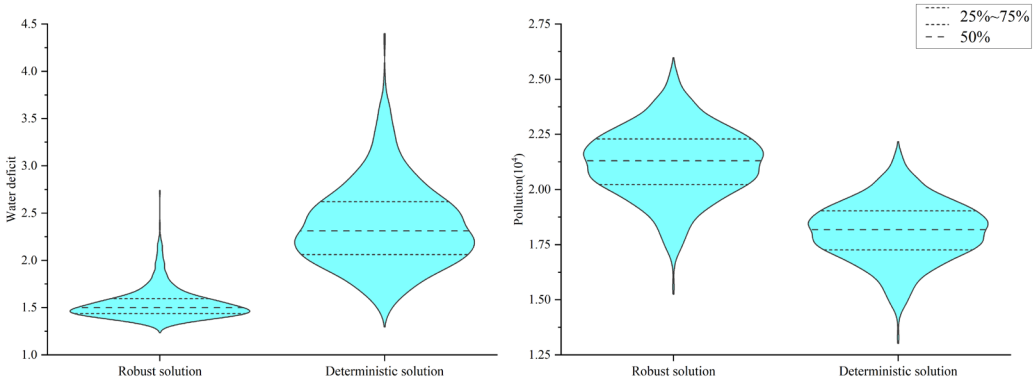

Figure 11. The integrated robustness index distribution of the robust and deterministic solution.

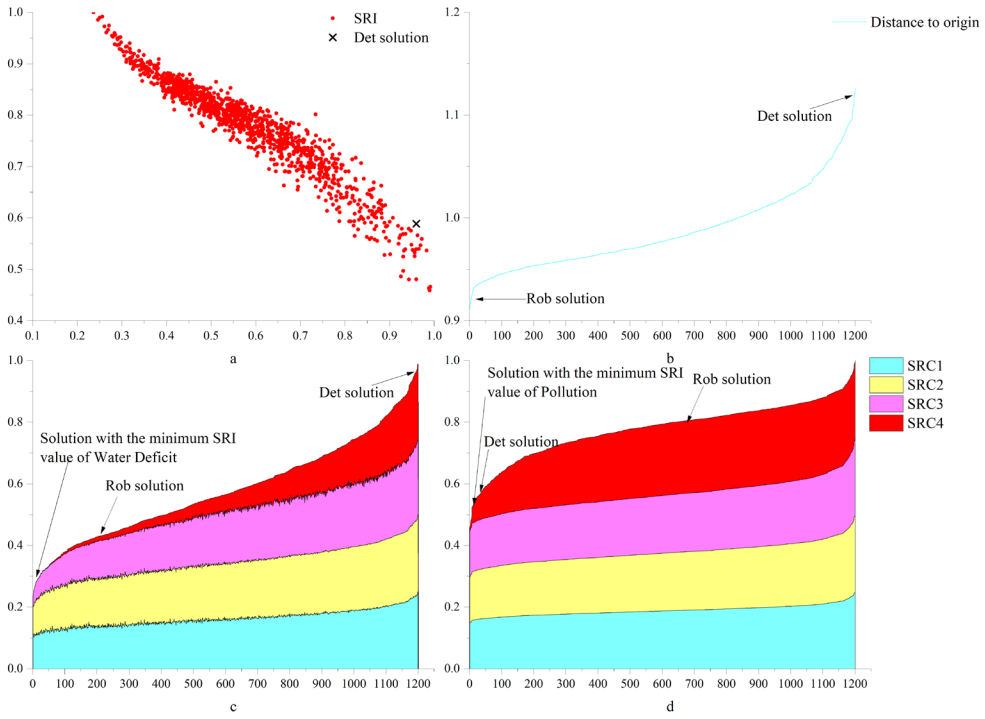

Figure 12. Comprehensive robustness criteria performance (a: Performance of comprehensive robustness criterion, b: Comprehensive robustness of robust solutions and deterministic solution, c and d: comprehensive robustness criteria for water deficit and pollution).

As shown in Figure 11, for water scarcity, the integrated criteria of the robust solution is clustered at approximately 0.5 and is significantly more robust than the deterministic solution; for pollution, the integrated index of the robust solution is significantly higher than that of the deterministic solution, but the span of the integrated index of the two solutions is similar, so the robustness of the deterministic solution is slightly better than that of the robust solution.

Similarly, as shown in Figure 12, there is also a Pareto front for the composite robustness criteria. For water deficit, the robustness of the robust solution is better than the deterministic solution; for pollution, the robustness of the deterministic solution is better than the robust solution. Specifically, for water deficit, the robust solution outperforms 85.3% of the solutions while the deterministic solution outperforms only about 1% of the solutions; for pollution, the deterministic solution outperforms 96% of the solutions while the robust solution outperforms only 39.6% of the solutions. According to the ratio of $SRI(Rob)/SRI(Det)$, the deterministic solution is about 130% more uncertain than the robust solution for water deficit; for pollution, the robust solution is about 37.7% more variable than the deterministic solution. The distance of each solution to the origin can reflect the comprehensive performance of the robustness of each solution. For the robustness composite index, the ratio of $Dis(Rob)/Dis(Det)$ is 0.655, which means that the composite robustness of the robust solution is 52.6% higher than the robustness of the deterministic solution.

For the robustness composite, the robust solution outperforms all the solutions, while the deterministic model solution outperforms only about 3.2% of the solutions. Comparing the distance to the origin of the robust solution and the deterministic solution, we can find that the robustness of the robust solution improves by 27.8% over the deterministic solution.

4.6 Analysis of specific water resources allocation schemes

First, as shown in Figure 13, we analyzed the proportion of water supply for each city. We find that the water supply share for the scheme most robust to water deficit rates is significantly higher than that for the scheme with the most robust pollutant emissions. This is because an increase in water supply leads to an increase in pollutant emissions, which in turn leads to a decrease in the robustness of pollutant emissions. For specific cities, the least robust allocation scenario for water deficit reduces the water supply in City 3, City 7, City 10, City 12, and City 15 compared to the most robust allocation scenario for pollutant emissions. Interestingly, these cities have the most water demand in the basin (as shown in Figure 3). Therefore, basin managers can increase the water supply to these cities if they need to improve the water deficit robustness of the water resources allocation scheme.

Then we analyze specifically the distribution of water resources between sectors. An interesting phenomenon can be observed. As shown in Figure 13, although the scenario with the best robustness in terms of pollutant emissions has a lower water supply than the scenario with the best robustness in terms of water deficit, the reduction is mainly in the agricultural sector. Water for domestic and industrial production did not change much. The reason for this may be that agricultural water use causes more pollution and may create more uncertainty. So how can watershed managers hope that improving the robustness of pollutant discharge can reduce water supply to the agricultural sector.

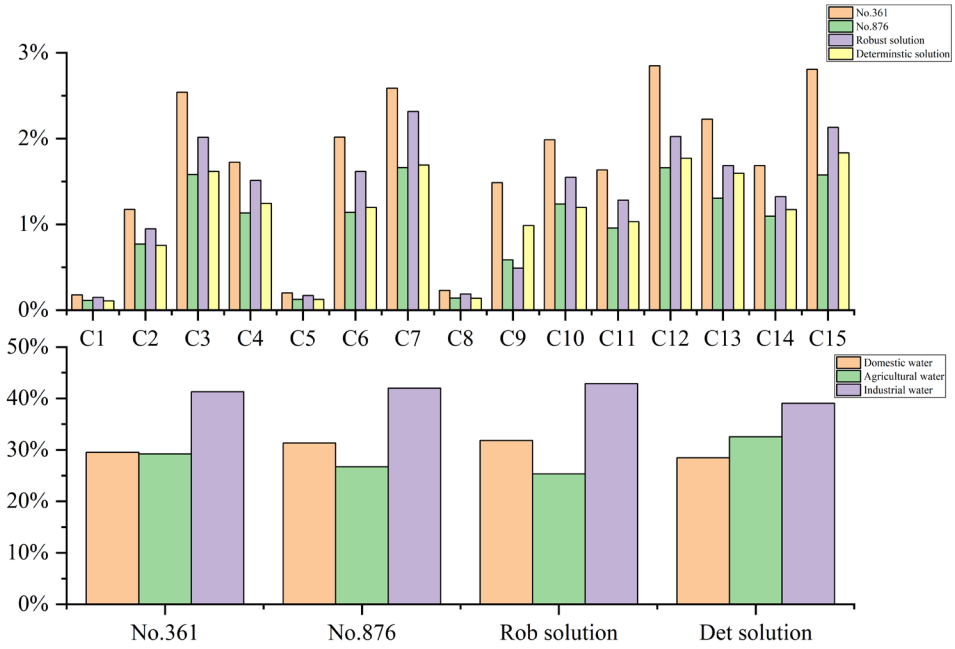

Figure 13. Specific water resources allocation schemes.

5. Conclusion

In this study, we propose a multi-objective robustness analysis method considering multiple uncertainties (CM-ROPAR approach) based on the robust optimization method for uncertainty perception (ROPAR approach). To verify the superiority and practicality of the CM-ROPAR approach, four robustness criteria are selected, and we compare the robust solution calculated by the method with the optimal solution of the deterministic model. In the studied case, there is a competitive relationship between the robustness of the two objective functions, which can form a Pareto frontier. For the water deficit rate, the robust solution outperforms the deterministic solution by 53%, 59%, 162%, and 1167% for the four robustness criteria, respectively; for the pollutant emission, the deterministic solution outperforms the robust

solution by only 17% for $RC1-RC3$, and outperforms the robust solution by 137% for $RC4$. For the composite robustness, the robust solution outperforms the deterministic solution by 52.6%, the CM-ROPAR finds a more robust solution.

The CM-ROPAR approach permits to exhibit the handling of uncertainty, to be able to analyze how uncertainty is transmitted to the Pareto frontier, and to perform the corresponding probabilistic analysis. The novelty of the new method compared to existing ROPAR methods is reflected in two aspects. First, the ROPAR method only considers uncertainty at a single point. In contrast, the CM-ROPAR method considers multiple uncertainties through the joint probability distribution of two points, which is closer to the actual situation and more general. Second, the new way analyzes the robustness of two objective functions of the solution instead of fixing one objective function to analyze the robustness of the other objective function. The CM-ROPAR method is more comprehensive and can identify the robustness of both objective functions, giving decision-makers more information for decision making.

One of the limitations of this study is that the CM-ROPAR approach is applicable to problems with two uncertainties and two objective functions; however, water allocation allows for more uncertainties and more objective functions (e.g., the uncertainty of inflow between multiple tributaries). In future research, we will focus on more complex objective functions and multi-objective optimization problems with at least three objective functions.

Author contribution. JZ and DS conceptualized the study and wrote the paper. ZD provided the data. All the authors took part in the interpretation of the results and edits of the paper.

Competing interests. The authors declare that they have no conflict of interest.

Acknowledgements. The authors are grateful to the Huaihe River Basin Management Committee for providing valuable economic and hydrological data. The authors are also grateful to the insight and views of the reviewers and editors. This research was supported by the Water Resources Department of Jiangsu Province (105012014-2023-054), the National key research and development program of China (2016YFC0401306) and National Natural Science Foundation of China Youth Science Fund Project (52309029).

Reference

Abdulbaki, D., Al-Hindi, M., Yassine, A., and Abou Najm, M.: An optimization model for the allocation of water resources, Journal of Cleaner Production, 164, 994-1006, 10.1016/j.jclepro.2017.07.024, 2017.

Ashofteh, P. S., Haddad, O. B., and A. Mariño, M.: Climate Change Impact on Reservoir Performance Indexesin Agricultural Water Supply, Journal of Irrigation and Drainage Engineering, 139, 85-97, 10.1061/(asce)ir.1943-4774.0000496, 2013.

Beyer, H.-G. and Sendhoff, B.: Robust optimization – A comprehensive survey, Computer Methods in Applied Mechanics and Engineering, 196, 3190-3218, 10.1016/j.cma.2007.03.003, 2007.

Chen, L., Xu, L., and Yang, Z.: Accounting carbon emission changes under regional industrial transfer in an urban agglomeration in China's Pearl River Delta, Journal of Cleaner Production, 167, 110-119, 10.1016/j.jclepro.2017.08.041, 2017.

Dong, Y. and Xu, L.: Aggregate risk of reactive nitrogen under anthropogenic disturbance in the Pearl River Delta urban agglomeration, Journal of Cleaner Production, 211, 490-502,

10.1016/j.jclepro.2018.11.194, 2019.
Habibi Davijani, M., Banihabib, M. E., Nadjafzadeh Anvar, A., and Hashemi, S. R.: Multi-Objective Optimization Model for the Allocation of Water Resources in Arid Regions Based on the Maximization of Socioeconomic Efficiency, Water Resources Management, 30, 927-946, 10.1007/s11269-015-1200-y, 2016.
Hassanzadeh, E., Elshorbagy, A., Wheater, H., and Gober, P.: A risk-based framework for water resource management under changing water availability, policy options, and irrigation expansion, Advances in Water Resources, 94, 291-306, 10.1016/j.advwatres.2016.05.018, 2016.
Jin, S. W., Li, Y. P., Yu, L., Suo, C., and Zhang, K.: Multidivisional planning model for energy, water and environment considering synergies, trade-offs and uncertainty, Journal of Cleaner Production, 259, 10.1016/j.jclepro.2020.121070, 2020.
Kang, D. and Lansey, K.: Scenario-Based Robust Optimization of Regional Water and Wastewater Infrastructure, Journal of Water Resources Planning and Management, 139, 325-338, 10.1061/(asce)wr.1943-5452.0000236, 2013.
Kapelan, Z., Savic, D. A., Walters, G. A., and Babayan, A. V.: Risk- and robustness-based solutions to a multi-objective water distribution system rehabilitation problem under uncertainty, Water Sci Technol, 53, 61-75, 10.2166/wst.2006.008, 2006.
Kapelan, Z. S., Savic, D. A., and Walters, G. A.: Multiobjective design of water distribution systems under uncertainty, Water Resources Research, 41, 10.1029/2004wr003787, 2005.
Keath, N. A. and Brown, R. R.: Extreme events: being prepared for the pitfalls with progressing sustainable urban water management, Water Sci Technol, 59, 1271-1280, 10.2166/wst.2009.136, 2009.
Li, M., Fu, Q., Singh, V. P., Liu, D., and Gong, X.: Risk-based agricultural water allocation under multiple uncertainties, Agricultural Water Management, 233, 10.1016/j.agwat.2020.106105, 2020.
Lu, H., Ren, L., Chen, Y., Tian, P., and Liu, J.: A cloud model based multi-attribute decision making approach for selection and evaluation of groundwater management schemes, Journal of Hydrology, 555, 881-893, 10.1016/j.jhydrol.2017.10.009, 2017.
Ma, Y., Li, Y. P., and Huang, G. H.: A bi-level chance-constrained programming method for quantifying the effectiveness of water-trading to water-food-ecology nexus in Amu Darya River basin of Central Asia, Environ Res, 183, 109229, 10.1016/j.envres.2020.109229, 2020.
Marchi, A., Dandy, G. C., and Maier, H. R.: Integrated Approach for Optimizing the Design of Aquifer Storage and Recovery Stormwater Harvesting Schemes Accounting for Externalities and Climate Change, Journal of Water Resources Planning and Management, 142, 10.1061/(asce)wr.1943-5452.0000628, 2016.
Marquez Calvo, O. O., Quintiliani, C., Alfonso, L., Di Cristo, C., Leopardi, A., Solomatine, D., and de Marinis, G.: Robust optimization of valve management to improve water quality in WDNs under demand uncertainty, Urban Water Journal, 15, 943-952, 10.1080/1573062x.2019.1595673, 2019.
Nelsen, R. B., Quesada-Molina, J. J., Rodríguez-Lallena, J. A., and Úbeda-Flores, M.: On the construction of copulas and quasi-copulas with given diagonal sections, Insurance: Mathematics and Economics, 42, 473-483, 10.1016/j.insmatheco.2006.11.011, 2008.
Nikoo, M. R., Kerachian, R., Karimi, A., and Azadnia, A. A.: Optimal water and waste-load allocations in rivers using a fuzzy transformation technique: a case study, Environ Monit Assess, 185, 2483-2502, 10.1007/s10661-012-2726-6, 2013.
Quintiliani, C., Marquez-Calvo, O., Alfonso, L., Di Cristo, C., Leopardi, A., Solomatine, D. P., and de

Marinis, G.: Multiobjective Valve Management Optimization Formulations for Water Quality Enhancement in Water Distribution Networks, Journal of Water Resources Planning and Management, 145, 10.1061/(asce)wr.1943-5452.0001133, 2019.
Reed, P. M., Hadka, D., Herman, J. D., Kasprzyk, J. R., and Kollat, J. B.: Evolutionary multiobjective optimization in water resources: The past, present, and future, Advances in Water Resources, 51, 438-456, 10.1016/j.advwatres.2012.01.005, 2013.
Ren, C., Li, Z., and Zhang, H.: Integrated multi-objective stochastic fuzzy programming and AHP method for agricultural water and land optimization allocation under multiple uncertainties, Journal of Cleaner Production, 210, 12-24, 10.1016/j.jclepro.2018.10.348, 2019.
Salvadori, G., Michele, C. D., Kottegoda, N. T., and Rosso, R.: Extremes in Nature: An Approach Using Copulas, Springer, Berlin2007.
Solomatine, D.: An approach to multi-objective robust optimization allowing for explicit analysis of robustness, https://www.un-ihe.org/sites/default/files/solomatine-ropar.pdf, 2012.
Solomatine, D. P. and Marquez-Calvo, O. O.: Approach to robust multi-objective optimization and probabilistic analysis: the ROPAR algorithm, Journal of Hydroinformatics, 21, 427-440, 10.2166/hydro.2019.095, 2019.
Sun, S., Fu, G., Bao, C., and Fang, C.: Identifying hydro-climatic and socioeconomic forces of water scarcity through structural decomposition analysis: A case study of Beijing city, Sci Total Environ, 687, 590-600, 10.1016/j.scitotenv.2019.06.143, 2019.
Xiong, W., Li, Y., Pfister, S., Zhang, W., Wang, C., and Wang, P.: Improving water ecosystem sustainability of urban water system by management strategies optimization, J Environ Manage, 254, 109766, 10.1016/j.jenvman.2019.109766, 2020.
Xu, Z., Pan, B., Han, M., Zhu, J., and Tian, L.: Spatial–temporal distribution of rainfall erosivity, erosivity density and correlation with El Niño–Southern Oscillation in the Huaihe River Basin, China, Ecological Informatics, 52, 14-25, 10.1016/j.ecoinf.2019.04.004, 2019.
Yang, W., Li, X., Sun, T., Pei, J., and Li, M.: Macrobenthos functional groups as indicators of ecological restoration in the northern part of China's Yellow River Delta Wetlands, Ecological Indicators, 82, 381-391, 10.1016/j.ecolind.2017.06.057, 2017.
Yazdi, J., Lee, E. H., and Kim, J. H.: Stochastic Multiobjective Optimization Model for Urban Drainage Network Rehabilitation, Journal of Water Resources Planning and Management, 141, 10.1061/(asce)wr.1943-5452.0000491, 2015.
Yu, S. and Lu, H.: An integrated model of water resources optimization allocation based on projection pursuit model – Grey wolf optimization method in a transboundary river basin, Journal of Hydrology, 559, 156-165, 10.1016/j.jhydrol.2018.02.033, 2018.
Zeng, X., Zhao, J., Wang, D., Kong, X., Zhu, Y., Liu, Z., Dai, W., and Huang, G.: Scenario analysis of a sustainable water-food nexus optimization with consideration of population-economy regulation in Beijing-Tianjin-Hebei region, Journal of Cleaner Production, 228, 927-940, 10.1016/j.jclepro.2019.04.319, 2019.
Zhu, F., Zhong, P.-a., Cao, Q., Chen, J., Sun, Y., and Fu, J.: A stochastic multi-criteria decision making framework for robust water resources management under uncertainty, Journal of Hydrology, 576, 287-298, 10.1016/j.jhydrol.2019.06.049, 2019.
Zhuang, X. W., Li, Y. P., Nie, S., Fan, Y. R., and Huang, G. H.: Analyzing climate change impacts on water resources under uncertainty using an integrated simulation-optimization approach, Journal of Hydrology, 556, 523-538, 10.1016/j.jhydrol.2017.11.016, 2018.

561